

# Possible $\Sigma^*(\frac{1}{2}^-)$ in initial-state polarized $\gamma N \rightarrow K^+\Sigma^*(1385) \rightarrow K^+\pi\Lambda$ reaction near threshold

Yun-Hua Chen<sup>1</sup> and B. S. Zou<sup>1,2</sup>

<sup>1</sup> *Institute of High Energy Physics, CAS,  
P.O. Box 918(4), Beijing 100049, China.*

<sup>2</sup> *State Key Laboratory of Theoretical Physics,  
Institute of Theoretical Physics, CAS, Beijing 100190, China.*

By using effective Lagrangian method, we study the effects of a newly proposed  $\Sigma^*(\frac{1}{2}^-)$  state with mass around 1380 MeV in initial-state polarized  $\gamma N \rightarrow K^+\Sigma^*(1385) \rightarrow K^+\pi\Lambda$  process near threshold. The theoretical predictions for the helicity cross sections  $\sigma_{\frac{3}{2}}, \sigma_{\frac{1}{2}}$  as well as their ratios, and the angular distributions of  $\pi$  in the  $\pi\Lambda$  c.m. system are given. It is found that assuming  $\Sigma^*(\frac{1}{2}^-)$  exists or not, these physical quantities are distinctly different. So our results could be useful for the investigation of the existence of  $\Sigma^*(\frac{1}{2}^-)$  when the experimental data are available in the future.

PACS numbers: 14.20.Jn, 25.20.Lj, 13.60.Le, 13.60.Rj

## I. INTRODUCTION

From studies of baryon spectroscopy and internal structures, the picture of some baryons have large five quark  $qqqq\bar{q}$  fraction was proposed [1–5]. The penta-quark picture can naturally solve some puzzles in classic three constituent quark models, for example for the  $J^P = \frac{1}{2}^-$  baryons why  $N^*(1535)$  is heavier than  $\Lambda^*(1405)$  [2]. For the lowest mass strange baryon, the penta-quark models [1, 6] predict a  $\Sigma^*(\frac{1}{2}^-)$  state with mass about 1360~1405 MeV which is around the mass, 1385 MeV, of the known  $\Sigma^*(\frac{3}{2}^+)$ . The studies of  $\Sigma^*$  are of intrinsic interest to check the correctness of penta-quark models, and recently some evidences for the existence of the  $\Sigma^*(\frac{1}{2}^-)$  near 1380 MeV have been found through research on the  $K^-p \rightarrow \Lambda\pi^+\pi^-$  process [7, 8],  $K\Lambda\pi$  [9] and  $K\Sigma\pi$  [10] photo-production processes.

Photo-production of  $K\Sigma^*$  provides a useful tool for understanding baryon spectroscopy and structures. While in the early time the limited experimental data on the cross section for  $\gamma + p \rightarrow K^+ + \Sigma^{*0}(1385)$  have large error bars [11–13]. Only in recent years, the high statistical experimental data on the  $K\Sigma^*$  photo-production have been made available. The CLAS Collaboration has measured the cross section of  $\gamma + p \rightarrow K^+ + \Sigma^{*0}(1385)$  with photon energies covering from the threshold up to 4.0 GeV [14]. The LEPS Collaboration has reported the first measurement

of the cross section and beam asymmetries of  $\gamma + n \rightarrow K^+ + \Sigma^{*-}(1385)$  process, using a linearly polarized photon beam with energy of  $E_\gamma = 1.5 - 2.4$  GeV [15]. Theoretical investigations of  $K\Sigma^*$  photo-production have been presented in Refs. [9, 16–18]. In Ref. [18], the t-, s- and u-channel diagrams as well as the contact term, which are required by gauge invariance, are calculated and are compared with the CLAS data [14]. Though the Ref. [18]’s theoretical results of the  $K\Sigma^*$  photo-production cross section agree well with the CLAS data and LEPS data, its prediction for the beam asymmetries greatly deviates from the measurement by LEPS Collaboration. This obstacle can be solved by including a new  $\Sigma^*(\frac{1}{2}^-)$  state with a mass around 1380 MeV, and in this way the experimental data from both CLAS Collaboration and LEPS Collaboration can be well described as found in Ref. [9].

The existence of  $\Sigma^*(\frac{1}{2}^-)$  can also be tested through the experimental measurement of initial-state polarized  $\gamma N \rightarrow K^+\Sigma^* \rightarrow K^+\pi\Lambda$  process. With the photon circularly polarized and the target of nucleon polarized both along the photon momentum direction, the total helicity may be  $\frac{3}{2}$  or  $\frac{1}{2}$ , which corresponding to spin-parallel and spin-antiparallel state of photon and nucleon respectively. In the energy range near threshold, the state of total helicity  $\frac{3}{2}$  can only produce  $\Sigma^*(\frac{3}{2}^+)$ , while the the state of total helicity  $\frac{1}{2}$  can produce both  $\Sigma^*(\frac{3}{2}^+)$  and  $\Sigma^*(\frac{1}{2}^-)$ . Theoretically, we can predict the helicity cross section  $\sigma_{\frac{3}{2}}$ ,  $\sigma_{\frac{1}{2}}$  and the angular distribution of the final  $\pi$  in the  $\pi\Lambda$  center-of-mass system assuming there only exist  $\Sigma^*(\frac{3}{2}^+)$  or there exist both  $\Sigma^*(\frac{3}{2}^+)$  and  $\Sigma^*(\frac{1}{2}^-)$ . The ratio of  $\frac{\sigma_{\frac{3}{2}}}{\sigma_{\frac{1}{2}}}$  and the angular distribution of  $\pi$  will be different in the two cases, so the existence of  $\Sigma^*(\frac{1}{2}^-)$  can be tested by future experimental analyses. In this article, within the framework of gauge-invariant effective Lagrangian from [9, 18] we have made such calculation of the initial-state polarized  $\gamma N \rightarrow K^+\Sigma^* \rightarrow K^+\pi\Lambda$  process taking into account or neglecting the  $\Sigma^*(\frac{1}{2}^-)$ .

This paper is organized as follows. In Sec. II, the theoretical framework is presented for the initial-state polarized  $\gamma N \rightarrow K^+\Sigma^* \rightarrow K^+\pi\Lambda$  process, where  $\Sigma^*$  include  $\Sigma^*(\frac{3}{2}^+)$  and  $\Sigma^*(\frac{1}{2}^-)$ . In Sec. III, the theoretical predictions for the helicity cross sections  $\sigma_{\frac{3}{2}}$ ,  $\sigma_{\frac{1}{2}}$  as well as their ratio, and the angular distribution of the  $\pi$  in the  $\pi\Lambda$  c.m. system with or without the  $\Sigma^*(\frac{1}{2}^-)$  are presented. We compare and discuss the results of these two cases. In Sec. IV, we give a summary of this work.

## II. THEORETICAL FRAMEWORK

The Feynman diagrams for  $\gamma N \rightarrow K^+\Sigma^* \rightarrow K^+\pi\Lambda$  are shown in Fig. 1, where  $k$ ,  $p$ ,  $q$ ,  $p_\pi$  and  $p_\Lambda$  are the momenta of incoming photon, nucleon and outgoing  $K$ ,  $\pi$ ,  $\Lambda$  respectively, and  $p'$  is the momentum of the intermediate  $\Sigma^*$ . Following the strategy of Ref. [9, 18], for the reaction

$\gamma N \rightarrow K^+ \Sigma^*(\frac{3}{2}^+) \rightarrow K^+ \pi \Lambda$  we consider the contribution of t-channel  $K$  meson exchange, the s-channel  $N$  and  $\Delta$  as well as their resonances exchange, the u-channel  $\Lambda$  (for the neutral propagator only) and  $\Sigma^*(\frac{3}{2}^+)$  exchange and the contact term. For the reaction  $\gamma N \rightarrow K^+ \Sigma^*(\frac{1}{2}^-) \rightarrow K^+ \pi \Lambda$ , we consider the contribution of t-channel  $K$  meson exchange, the s-channel  $N$  exchange, the u-channel  $\Sigma^*(\frac{1}{2}^-)$  exchange (and  $\Lambda$  exchange for  $\gamma p \rightarrow K^+ \Sigma^{*0}(\frac{1}{2}^-)$ ) and the contact term.

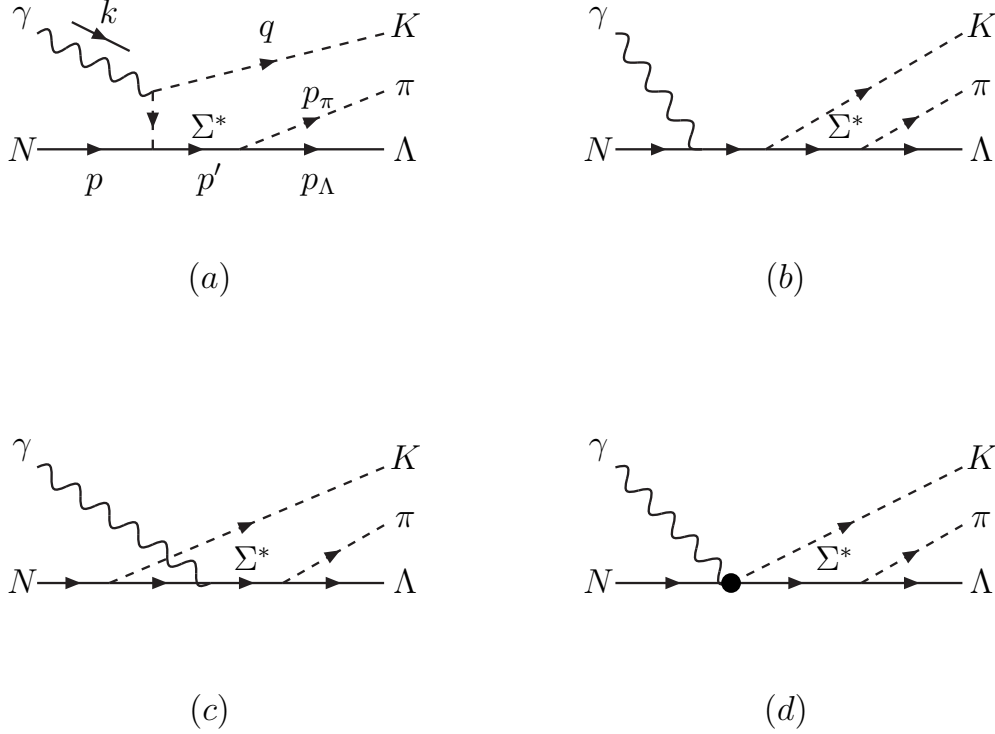


FIG. 1: Feynman diagrams for  $\gamma N \rightarrow K^+ \Sigma^* \rightarrow K^+ \pi \Lambda$ . (a) t-channel; (b) s-channel; (c) u-channel; (d) contact term.

The effective Lagrangians and coupling constants relevant to the  $\gamma N \rightarrow K^+ \Sigma^*$  reaction used in this article are taken from Ref. [9, 18], which are listed below for completeness, and the interested reader can consult Ref. [9, 18] for more details.

For the t-channel  $K$  meson exchange:

$$\mathcal{L}_{\gamma KK} = ieA_\mu (K^- \partial^\mu K^+ - \partial^\mu K^- K^+), \quad (1)$$

$$\mathcal{L}_{KN\Sigma_{3/2}^*} = \frac{f_{KN\Sigma_{3/2}^*}}{m_K} \partial_\mu \bar{K} \bar{\Sigma}_{3/2}^{*\mu} \cdot \tau N + \text{H.c.}, \quad (2)$$

$$\mathcal{L}_{KN\Sigma_{1/2}^*} = -ig_{KN\Sigma_{1/2}^*} \bar{K} \bar{\Sigma}_{1/2}^* \cdot \tau N + \text{H.c.}, \quad (3)$$

with the isospin structure of  $K\Sigma^*N$  coupling,

$$\bar{K} = (K^-, \bar{K}^0), \bar{\Sigma}^* \cdot \tau = \begin{pmatrix} \bar{\Sigma}^{*0} & \sqrt{2}\bar{\Sigma}^{*+} \\ \sqrt{2}\bar{\Sigma}^{*-} & -\bar{\Sigma}^{*0} \end{pmatrix}, N = \begin{pmatrix} p \\ n \end{pmatrix}, \quad (4)$$

where the coupling constant  $f_{KN\Sigma_{3/2}^*} = -3.22$  [18] and  $g_{KN\Sigma_{1/2}^*} = 1.34$  [9].

For the s-channel of nucleon exchange, the effective Lagrangian for  $\gamma NN$  vertex is

$$\mathcal{L}_{\gamma NN} = -e\bar{N}(\gamma^\mu A_\mu Q_N - \frac{\kappa_N}{2M_N}\sigma^{\mu\nu}\partial_\nu A_\mu)N, \quad (5)$$

where  $Q_N$  is the electric charge (in unite of  $e$ ), and  $\kappa_N$  denotes the magnetic moment of the nucleon:  $\kappa_n = -1.913$  and  $\kappa_p = 2.793$ .

The  $\gamma N \rightarrow K^+\Sigma^*(\frac{3}{2}^+)$  process has s-channel spin- $\frac{3}{2}$  and spin- $\frac{5}{2}$  resonances exchange diagrams, and the effective Lagrangians are

$$\mathcal{L}_{\gamma NR}(\frac{3^\pm}{2}) = -\frac{ief_1}{2M_N}\bar{N}\Gamma_\nu^{(\pm)}F^{\mu\nu}R_\mu - \frac{ef_2}{(2M_N)^2}\partial_\nu\bar{N}\Gamma^{(\pm)}F^{\mu\nu}R_\mu + \text{H.c.}, \quad (6)$$

$$\mathcal{L}_{\gamma NR}(\frac{5^\pm}{2}) = \frac{ef_1}{(2M_N)^2}\bar{N}\Gamma_\nu^{(\mp)}\partial^\alpha F^{\mu\nu}R_{\mu\alpha} - \frac{ief_2}{(2M_N)^3}\partial_\nu\bar{N}\Gamma^{(\mp)}\partial^\alpha F^{\mu\nu}R_{\mu\alpha} + \text{H.c.}, \quad (7)$$

and

$$\mathcal{L}_{RK\Sigma^*}(\frac{3^\pm}{2}) = \frac{h_1}{m_K}\partial^\alpha K\bar{\Sigma}^{*\mu}\Gamma_\alpha^{(\pm)}R_\mu + \frac{ih_2}{(m_K)^2}\partial^\mu\partial^\alpha K\bar{\Sigma}_\alpha^*\Gamma^{(\pm)}R_\mu + \text{H.c.}, \quad (8)$$

$$\mathcal{L}_{RK\Sigma^*}(\frac{5^\pm}{2}) = \frac{ih_1}{m_K^2}\partial^\mu\partial^\beta K\bar{\Sigma}^{*\alpha}\Gamma_\mu^{(\mp)}R_{\alpha\beta} - \frac{h_2}{(m_K)^3}\partial^\mu\partial^\alpha\partial^\beta K\bar{\Sigma}_\mu^*\Gamma^{(\mp)}R_{\alpha\beta} + \text{H.c.}, \quad (9)$$

where  $F^{\mu\nu} = \partial^\mu A^\nu - \partial^\nu A^\mu$ ,  $R_\mu$  and  $R_{\mu\alpha}$  denote the spin- $\frac{3}{2}$  and spin- $\frac{5}{2}$  fields, respectively, and

$$\Gamma_\mu^{(\pm)} = \begin{pmatrix} \gamma_\mu\gamma_5 \\ \gamma_\mu \end{pmatrix}, \Gamma^{(\pm)} = \begin{pmatrix} \gamma_5 \\ 1 \end{pmatrix}. \quad (10)$$

For the  $\Delta$  resonances of isospin- $\frac{3}{2}$ , the effective Lagrangians have the isospin structure

$$\begin{aligned} \bar{K}\bar{\Sigma}^* \cdot \mathbf{T}(\frac{1}{2}, \frac{3}{2})\Delta &= \sqrt{3}K^-\bar{\Sigma}^{*+}\Delta^{++} - \sqrt{2}K^-\bar{\Sigma}^{*0}\Delta^+ - K^-\bar{\Sigma}^{*-}\Delta^0 \\ &+ \bar{K}^0\bar{\Sigma}^{*+}\Delta^+ - \sqrt{2}\bar{K}^0\bar{\Sigma}^{*0}\Delta^0 - \sqrt{3}\bar{K}^0\bar{\Sigma}^{*-}\Delta^-. \end{aligned} \quad (11)$$

For the  $\gamma N\Delta$  coupling, we have  $f_1 = 4.04$  and  $f_2 = 3.87$ . For the  $\Delta K\Sigma^*$  coupling,  $h_1 = 2.0$  and  $h_2 = 0$  are obtained from  $h_1 = -f_{K\Delta\Sigma^*}/\sqrt{3}$  with  $f_{K\Delta\Sigma^*} = -3.46$  [19]. In addition we consider three PDG resonances in the s-channel,  $N_{\frac{3}{2}}^-(2080)$ ,  $\Delta_{\frac{3}{2}}^-(1940)$  and  $\Delta_{\frac{5}{2}}^+(2000)$  [20]. One has  $f_1 = -1.25$  and  $f_2 = 1.21$  for the  $\gamma p N^*(2080)$  coupling;  $f_1 = 0.381$  and  $f_2 = -0.256$  for the  $\gamma n N^*(2080)$  coupling;  $f_1 = 0.39$  and  $f_2 = -0.57$  for the  $\gamma N\Delta(1940)$  coupling, and  $f_1 = -0.68$ ,

$f_2 = -0.062$  for the  $\gamma N \Delta(2000)$  coupling. For the resonances coupling to  $K\Sigma^*$ , one has  $h_1 = 0.24$  and  $h_2 = -0.54$  for the  $N^*(2080)K\Sigma^*$  coupling,  $h_1 = -0.68$  and  $h_2 = 1.0$  for the  $\Delta(1940)K\Sigma^*$  coupling, and  $h_1 = -1.1$  and  $h_2 = 0.21$  for the  $\Delta(2000)K\Sigma^*$  coupling.

For the u-channel  $\Lambda(1116)$  exchange in the  $\gamma p \rightarrow K^+\Sigma^{*0}$  reaction, the effective Lagrangians are

$$\mathcal{L}_{\gamma\Lambda\Sigma_{3/2}^*} = -\frac{ief_1}{2M_\Lambda}\bar{\Lambda}\gamma_\nu\gamma_5 F^{\mu\nu}\Sigma_{3/2\mu}^* - \frac{ef_2}{(2M_\Lambda)^2}\partial_\nu\bar{\Lambda}\gamma_5 F^{\mu\nu}\Sigma_{3/2\mu}^* + \text{H.c.}, \quad (12)$$

$$\mathcal{L}_{\gamma\Lambda\Sigma_{1/2}^*} = \frac{eg_{\gamma\Lambda\Sigma_{1/2}^*}}{4(M_\Lambda + M_{\Sigma_{1/2}^*})}\bar{\Sigma}_{1/2}^*\gamma_5\sigma_{\mu\nu}\Lambda F^{\nu\mu} + \text{H.c.}, \quad (13)$$

$$\mathcal{L}_{KN\Lambda} = \frac{g_{KN\Lambda}}{M_N + M_\Lambda}\bar{N}\gamma^\mu\gamma_5\Lambda\partial_\mu K + \text{H.c.}, \quad (14)$$

where  $f_1 = 4.52$ ,  $f_2 = 5.63$  are obtained from the decay width  $\Gamma(\Sigma_{3/2}^* \rightarrow \Lambda\gamma)$  and  $g_{\gamma\Lambda\Sigma_{1/2}^*} = 1.16$ . From the flavor SU(3) symmetry relation, one has  $g_{KN\Lambda} = -13.24$  [18].

For the u-channel  $\Sigma^*$  exchange, the effective Lagrangians are

$$\mathcal{L}_{\gamma\Sigma_{1/2}^*\Sigma_{1/2}^*} = -e\bar{\Sigma}_{1/2}^*(\gamma^\mu A_\mu Q_{\Sigma_{1/2}^*} - \frac{\kappa_{\Sigma_{1/2}^*}}{2M_N}\sigma^{\mu\nu}\partial_\nu A_\mu)\Sigma_{1/2}^*, \quad (15)$$

$$\mathcal{L}_{\gamma\Sigma_{3/2}^*\Sigma_{3/2}^*} = e\bar{\Sigma}_{3/2\mu}^* A_\alpha \Gamma_{\gamma\Sigma_{3/2}^*}^{\alpha,\mu\nu} \Sigma_{3/2\nu}^*, \quad (16)$$

with

$$A_\alpha \Gamma_{\gamma\Sigma_{3/2}^*}^{\alpha,\mu\nu} = Q_{\Sigma_{3/2}^*} A_\alpha (g^{\mu\nu}\gamma^\alpha - \frac{1}{2}(\gamma^\mu\gamma^\nu\gamma^\alpha + \gamma^\alpha\gamma^\mu\gamma^\nu)) - \frac{\kappa_{\Sigma_{3/2}^*}}{2M_N}\sigma^{\alpha\beta}\partial_\beta A_\alpha g^{\mu\nu}, \quad (17)$$

where  $Q_{\Sigma^*}$  is the electric charge (in units of  $e$ ), and  $\kappa_{\Sigma^*}$  denotes the anomalous magnetic moment of  $\Sigma^*$ :  $\kappa_{\Sigma_{3/2}^{*0}} = 0.36$  and  $\kappa_{\Sigma_{3/2}^{*-}} = -2.43$  are taken from the quark model [21], and  $\kappa_{\Sigma_{1/2}^{*0}} = -0.43$  and  $\kappa_{\Sigma_{1/2}^{*-}} = -1.74$  are predicted by the penta-quark model [6].

To take account of the off-shell effects, every vertex of these channels has been given a form factor. For the t-channel  $K$  meson exchange, we use the form factor [18]

$$F_M = \frac{\Lambda_M^2 - m_K^2}{\Lambda_M^2 - q_t^2}, \quad (18)$$

where  $q_t = k - q$ . We adopt  $\Lambda_M = 0.83$  GeV for  $\Sigma_{3/2}^*$  and  $\Lambda_M = 1.6$  GeV for  $\Sigma_{1/2}^*$  respectively [9]. For s-channel  $N$  and  $\Delta$  exchange, the u-channel processes and the  $\Sigma^*\Lambda\pi$  vertex, we adopt the form factor [18]

$$F_B(q_{ex}^2, M_{ex}) = \frac{\Lambda_B^4}{\Lambda_B^4 + (q_{ex}^2 - M_{ex}^2)^2}, \quad (19)$$

where the  $q_{ex}$  and  $M_{ex}$  are the 4-momentum and the mass of the exchanged hadron, respectively. For s-channel resonances exchange, the form factor is

$$F_B(q_s^2, M_R) = \exp\left(-\frac{(q_s^2 - M_R^2)^2}{\Lambda_B^4}\right). \quad (20)$$

with the cutoff parameter  $\Lambda_B = 1.0$  GeV [18].

The contact term in Fig. 1 (d) is required to keep the full amplitude gauge invariant. For the process  $\gamma p \rightarrow K^+ \Sigma_{3/2}^{*0}$ , we adopt the contact current [18, 22]

$$M_c^{\mu\nu} = ie \frac{f_{KN\Sigma_{3/2}^*}}{m_K} (g^{\mu\nu} f_t - q^\mu C^\nu), \quad (21)$$

where  $C^\nu$  is expressed as

$$C^\nu = -(2q - k)^\nu \frac{f_t - 1}{t - m_K^2} (1 - h(1 - f_s)) - (2p + k)^\nu \frac{f_s - 1}{s - M_N^2} (1 - h(1 - f_t)). \quad (22)$$

Here the Lorenz index  $\mu$  and  $\nu$  couple to that of  $\Sigma_{3/2}^*$  and the photon respectively;  $f_t = F_M^2$  and  $f_s = F_B^2(s, M_N)$  are form factors squared, and  $t = q_t^2$  and  $s = q_s^2$ ;  $h$  is a parameter to be fitted to experiments, and  $h = 1$  is used in Ref.[18]. For the process  $\gamma p \rightarrow K^+ \Sigma_{1/2}^{*0}$ , the contact current is

$$M_c^\nu = ie g_{KN\Sigma_{1/2}^*} C^\nu, \quad (23)$$

where  $h = 1$  is adopted. For the reaction  $\gamma n \rightarrow K^+ \Sigma_{3/2}^{*-}$ , the contact current is [22]

$$M_c^{\mu\nu} = ie\sqrt{2} \frac{f_{KN\Sigma_{3/2}^*}}{m_K} (g^{\mu\nu} f_t - q^\mu C^\nu), \quad (24)$$

with

$$C^\nu = -(2q - k)^\nu \frac{f_t - 1}{t - m_K^2} (1 - h(1 - f_u)) + (2p' - k)^\nu \frac{f_u - 1}{u - M_{\Sigma^*}^2} (1 - h(1 - f_t)), \quad (25)$$

where  $f_u = F_B^2(u, M_{\Sigma^*}^2)$  is the form factor squared, and  $u = q_u^2$  is the squared momentum transfer for the u-channel. According to Ref. [9],  $h = 1.11$  is taken assuming there only exist  $\Sigma^*(\frac{3}{2}^+)$ , and  $h = 1$  is used if there exist both  $\Sigma^*(\frac{3}{2}^+)$  and  $\Sigma^*(\frac{1}{2}^-)$ . For  $\gamma n \rightarrow K^+ \Sigma^{*-}(\frac{1}{2}^-)$  process, we adopt the contact current:

$$M_c^\nu = ie\sqrt{2} g_{KN\Sigma_{1/2}^*} C^\nu, \quad (26)$$

where  $C^\nu$  is expressed as Eq.(25), and here  $h = 1$  is taken.

All the ingredients of  $\gamma N \rightarrow K^+ \Sigma^*$  reaction are given above, and now we list the effective Lagrangians of  $\Sigma^* \Lambda \pi$  vertex [8, 23]:

$$\mathcal{L}_{\Lambda\pi\Sigma_{3/2}^*} = g_{\Lambda\pi\Sigma_{3/2}^*} \bar{\Lambda} \Sigma_{3/2}^{*\mu} \partial_\mu \pi + \text{H.c.}, \quad (27)$$

$$\mathcal{L}_{\Lambda\pi\Sigma_{1/2}^*} = -ig_{\Lambda\pi\Sigma_{1/2}^*} \bar{\Sigma}_{1/2}^* \Lambda \pi + \text{H.c.}, \quad (28)$$

where  $g_{\Lambda\pi\Sigma_{3/2}^*} = 9.16$  is obtained from the decay widths of  $\Gamma(\Sigma_{3/2}^* \rightarrow \Lambda\pi)$  [20], and  $g_{\Lambda\pi\Sigma_{1/2}^*} = 2.12$  is obtained assuming the fitted result of the  $\Sigma_{1/2}^*$  decay width in Ref. [7] is contributed totally by the  $\Lambda\pi$  channel.

Further more, we need the propagators of intermediate particles to calculate the Feymann diagrams. For t-channel exchange  $K$  meson, the propagator is

$$G_{K(q_t)} = 1/(q_t^2 - m_K^2). \quad (29)$$

For the spin-1/2, spin-3/2 and spin -5/2 baryons the propagators are respectively

$$G_{R(p)}^{\frac{1}{2}} = \frac{\not{p} + m}{p^2 - m^2}, \quad (30)$$

$$G_{R(p)}^{\frac{3}{2}} = \frac{\not{p} + m}{p^2 - m^2} \left( -g^{\mu\nu} + \frac{\gamma^\mu \gamma^\nu}{3} + \frac{\gamma^\mu p^\nu - \gamma^\nu p^\mu}{3m} + \frac{2p^\mu p^\nu}{3m^2} \right), \quad (31)$$

$$G_{R(p)}^{\frac{5}{2}} = \frac{\not{p} + m}{p^2 - m^2} S_{\alpha\beta\mu\nu}(p, m), \quad (32)$$

where

$$S_{\alpha\beta\mu\nu}(p, m) = \frac{1}{2}(\bar{g}_{\alpha\mu}\bar{g}_{\beta\nu} + \bar{g}_{\alpha\nu}\bar{g}_{\beta\mu}) - \frac{1}{5}\bar{g}_{\alpha\beta}\bar{g}_{\mu\nu} - \frac{1}{10}(\bar{\gamma}_\alpha\bar{\gamma}_\mu\bar{g}_{\beta\nu} + \bar{\gamma}_\alpha\bar{\gamma}_\nu\bar{g}_{\beta\mu} + \bar{\gamma}_\beta\bar{\gamma}_\mu\bar{g}_{\alpha\nu} + \bar{\gamma}_\beta\bar{\gamma}_\nu\bar{g}_{\alpha\mu}) \quad (33)$$

with

$$\begin{aligned} \bar{g}_{\mu\nu} &= g_{\mu\nu} - \frac{p_\mu p_\nu}{m^2}, \\ \bar{\gamma}_\mu &= \gamma_\mu - \frac{p_\mu}{m^2} \not{p}. \end{aligned} \quad (34)$$

For the intermediate resonances with sizeable width  $\Gamma$ , namely  $N_{\frac{3}{2}^-}$ (2080),  $\Delta_{\frac{3}{2}^-}$ (1940),  $\Delta_{\frac{5}{2}^+}$ (2000),  $\Sigma^*(\frac{3}{2}^+)$  and  $\Sigma^*(\frac{1}{2}^-)$ , we replace the denominator  $\frac{1}{p^2 - m^2}$  in the propagators by  $\frac{1}{p^2 - m^2 + im\Gamma}$ , and replace  $m$  in the rest of the propagators by  $\sqrt{p^2}$ . These decay widths are taken from Ref. [7, 9], which are within the PDG range,  $\Gamma_{N^*(2080)} = 0.25$  GeV,  $\Gamma_{\Delta(1940)} = 0.15$  GeV,  $\Gamma_{\Delta(2000)} = 0.15$  GeV,  $\Gamma_{\Sigma^*(\frac{3}{2}^+)} = 0.035$  GeV and  $\Gamma_{\Sigma^*(\frac{1}{2}^-)} = 0.119$  GeV. Since previous investigation indicates the new  $\Sigma^*(\frac{1}{2}^-)$ 's mass is around  $\Sigma^*(\frac{3}{2}^+)$  [7-9], here we assume its mass be the same as  $\Sigma^*(\frac{3}{2}^+)$ .

The differential cross section for  $\gamma N \rightarrow K^+ \Sigma^* \rightarrow K^+ \pi \Lambda$  can be expressed as

$$d\sigma_{\gamma N \rightarrow K^+ \Sigma^* \rightarrow K^+ \pi \Lambda} = \frac{|\mathbf{q}| |\mathbf{p}_\pi| |\bar{\mathcal{M}}|^2}{(2\pi)^5 32s |\mathbf{k}|} d\Omega d\Omega' dm_{\pi\Lambda} \quad (35)$$

where  $\mathbf{k}$  and  $\mathbf{q}$  denote the 3-momenta of photon and  $K^+$  in the c.m. frame respectively, and  $\mathbf{p}_\pi$  is the 3-momenta of the produced  $\pi$  in the  $\Sigma^*$  rest frame;  $d\Omega = 2\pi d\cos\theta$ , and  $\theta$  denotes the angle of the outgoing  $K^+$  relative to beam direction in the c.m. frame;  $d\Omega' = d\cos\theta' d\phi'$  is the sphere space of the outgoing  $\pi$  in the  $\Sigma^*$  rest frame, and  $\theta'$  is the angle between the  $\pi$  direction and the

$K^+$  direction in the c.m system of the  $\pi\Lambda$ ;  $m_{\pi\Lambda}$  is the invariant mass of  $\pi$  and  $\Lambda$ , which satisfies  $m_{\pi\Lambda}^2 = (p_\pi + p_\Lambda)^2$ . With the z-axis being the direction of motion of the photon and the x-z plane being the reaction plane, the polarization vectors for right and left handed photons are

$$\vec{\epsilon}_R = -\frac{1}{\sqrt{2}}(\vec{\epsilon}_x + i\vec{\epsilon}_y), \quad \vec{\epsilon}_L = +\frac{1}{\sqrt{2}}(\vec{\epsilon}_x - i\vec{\epsilon}_y). \quad (36)$$

For the polarized nucleon we use the projection operators [24]

$$u(p)\bar{u}(p) = (\not{p} + m_N)\frac{1}{2}(1 + 2\lambda\gamma_5\not{\vec{p}}), \quad (37)$$

where  $\lambda = \pm\frac{1}{2}$  is the helicity of nucleon and  $s = (\frac{|\vec{p}|}{m_N}, \frac{E_N}{m_N} \frac{\vec{p}}{|\vec{p}|})$ .

### III. RESULTS AND DISCUSSIONS

With the formalism and ingredients given above, we compute the helicity cross section  $\sigma_{\frac{3}{2}}$  and  $\sigma_{\frac{1}{2}}$ , corresponding to spin-parallel and spin-antiparallel states of the photon and nucleon respectively, for the  $\gamma N \rightarrow K^+\Sigma^* \rightarrow K^+\pi\Lambda$  process assuming there only exists  $\Sigma^*(\frac{3}{2}^+)$  or there exist both  $\Sigma^*(\frac{3}{2}^+)$  and  $\Sigma^*(\frac{1}{2}^-)$ . The cross sections versus excess energy in c.m. frame,  $Q = \sqrt{s} - \sqrt{s_{threshold}}$ , are shown in Fig. 2, in which we also exhibit the contribution of  $\Sigma^*(\frac{1}{2}^-)$  for comparison. In Fig. 3, the behavior of the ratios of  $\sigma_{\frac{3}{2}}/\sigma_{\frac{1}{2}}$  are given.

Through analysis we find that the contact terms and the u-channel  $\Lambda$  exchange give the most important contributions to the  $\gamma p \rightarrow K^+\Sigma^{*0}(\frac{3}{2}^+) \rightarrow K^+\pi^0\Lambda$  process. While their interference term enhances and reduces the total cross section for  $\sigma_{\frac{3}{2}}$  and  $\sigma_{\frac{1}{2}}$  respectively, so the ratio of  $\sigma_{\frac{3}{2}}/\sigma_{\frac{1}{2}}$  for pure  $\Sigma^*(\frac{3}{2}^+)$  produced process is about 40 as in Fig. 3 (a). For the  $\gamma p \rightarrow K^+\Sigma^{*0}(\frac{1}{2}^-) \rightarrow K^+\pi^0\Lambda$  process,  $\sigma_{\frac{1}{2}}$  comes mainly from the t-channel  $K$  exchange and the s-channel  $N$  exchange, while in  $\sigma_{\frac{3}{2}}$  the s-channel  $N$  exchange's contribution is suppressed due to angular momentum conservation so  $\sigma_{\frac{1}{2}}$  is larger than  $\sigma_{\frac{3}{2}}$ . Assuming there exist both  $\Sigma^*(\frac{3}{2}^+)$  and  $\Sigma^*(\frac{1}{2}^-)$ , the ratio of  $\sigma_{\frac{3}{2}}/\sigma_{\frac{1}{2}}$  is about 3 which is distinct from that assuming only  $\Sigma^*(\frac{3}{2}^+)$  exist, which can be seen in Fig. 3 (a).

For the  $\gamma n \rightarrow K^+\Sigma^{*-}(\frac{3}{2}^+) \rightarrow K^+\pi^-\Lambda$  process, the contact term plays the major role and its contribution to the total cross section is two orders larger than those from other channels, so the ratio of  $\sigma_{\frac{3}{2}}/\sigma_{\frac{1}{2}}$  mainly depends on the behavior of the contact term. For the  $\gamma n \rightarrow K^+\Sigma^{*-}(\frac{1}{2}^-) \rightarrow K^+\pi^-\Lambda$  process, the major contribution is from the t-channel  $K$  exchange. As can be seen in Fig. 3 (a) and (b), the ratios of  $\sigma_{\frac{3}{2}}/\sigma_{\frac{1}{2}}$  from pure  $\Sigma^*(\frac{1}{2}^-)$  are zero at threshold as expected, while they sharply rise and reach about one when  $Q = 10$  MeV. This is because the amplitude of the major t-channel  $K$  exchange in  $\Sigma^*(\frac{1}{2}^-)$  produced reactions is proportional to the component of



the photon polarization vector parallel to the reaction plane, and its contributions to the total cross section are the same for right and left handed photons. As shown in Fig. 2 (b), the  $\Sigma^*(\frac{1}{2}^-)$  produced cross sections are larger than those produced by  $\Sigma^*(\frac{3}{2}^+)$ , so taking account of the  $\Sigma^*(\frac{1}{2}^-)$  or not, the total cross section will be different, both for  $\sigma_{\frac{3}{2}}$  or for  $\sigma_{\frac{1}{2}}$ . Also, in Fig. 3 (b), the ratios of  $\sigma_{\frac{3}{2}}/\sigma_{\frac{1}{2}}$  are different assuming there exist both  $\Sigma^*(\frac{3}{2}^+)$  and  $\Sigma^*(\frac{1}{2}^-)$  or only exist  $\Sigma^*(\frac{3}{2}^+)$ .

Another way to investigate the spin of the  $\Sigma^*$  is to utilize the angular distribution of the  $\pi$  in the  $\pi\Lambda$  center-of-mass system. Near threshold, the final  $\pi\Lambda$  state is in the relative  $p$  wave from the decay of  $\Sigma^*(\frac{3}{2}^+)$  and is in the relative  $s$  wave from the decay of  $\Sigma^*(\frac{1}{2}^-)$ . So the angular distribution is expected to be of the form  $(a + b \cos \theta'^2)$  for the pure  $\Sigma^*(\frac{3}{2}^+)$  and a flat constant distribution is predicted for pure  $\Sigma^*(\frac{1}{2}^-)$ . In Fig. 4 and Fig. 5, we show the angular distribution of the  $\pi$  in the  $\pi\Lambda$  center-of-mass system for the  $\gamma N \rightarrow K^+ \Sigma^* \rightarrow K^+ \pi \Lambda$  process assuming there exist only  $\Sigma^*(\frac{3}{2}^+)$  and there exist both  $\Sigma^*(\frac{3}{2}^+)$  and  $\Sigma^*(\frac{1}{2}^-)$  at  $Q=20$  MeV, respectively. Note that here we choose the energy  $Q=20$  MeV just as an example, and the behaviors of the angular distributions do not change significantly near threshold. As illustrated in Fig. 4, the shapes of angular distributions for pure  $\Sigma^*(\frac{3}{2}^+)$  agree well with the expectations. We also have checked that the predictions for the angular distributions from pure  $\Sigma^*(\frac{1}{2}^-)$  are flat constants, and we do not illustrate them individually in the figures. The differential cross section contributed by the interference terms of the  $\Sigma^*(\frac{3}{2}^+)$  and  $\Sigma^*(\frac{1}{2}^-)$  are linear functions of  $\cos \theta'$ , and we find they change much rapidly than the corresponding pure  $\Sigma^*(\frac{3}{2}^+)$  terms in the  $\gamma p \rightarrow K^+ \Sigma^{*0} \rightarrow K^+ \pi^0 \Lambda$  process for  $\sigma_{3/2}$ , and in the  $\gamma n \rightarrow K^+ \Sigma^{*-} \rightarrow K^+ \pi^- \Lambda$  process for  $\sigma_{3/2}$  and  $\sigma_{1/2}$ , so in these reactions the interference terms mainly determine the shapes of the angular distributions as shown in Fig. 5 (a),(c) and (d). In the  $\gamma p \rightarrow K^+ \Sigma^{*0} \rightarrow K^+ \pi^0 \Lambda$  process for  $\sigma_{1/2}$ , the interference term changes more slowly than the pure  $\Sigma^*(\frac{3}{2}^+)$  term so the shape of the angular distribution deviates slightly from that of pure  $\Sigma^*(\frac{3}{2}^+)$ , as can be seen in Fig. 5 (b).

#### IV. SUMMARY

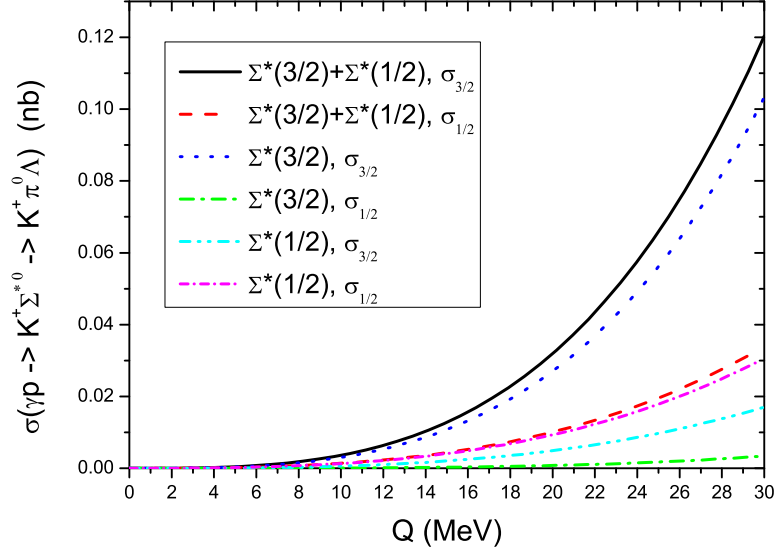
In this paper, we study the reactions  $\gamma N \rightarrow K^+ \Sigma^*(1385) \rightarrow K^+ \pi \Lambda$  near threshold within an effective Lagrangian approach. Recent studies indicate that near the mass of  $\Sigma^*(\frac{3}{2}^+)$ , another  $\Sigma^*$  state with  $J^P = \frac{1}{2}^-$  may exist. The spin of  $\Sigma^*$  can be investigated in  $K \Sigma^*$  photo-production process using circularly polarized photons and a target of polarized nucleons. Taking account of the  $\Sigma^*(\frac{1}{2}^-)$  or not, we compute the helicity cross sections  $\sigma_{\frac{3}{2}}$  and  $\sigma_{\frac{1}{2}}$ , which correspond to spin-parallel and spin-antiparallel states of the photon and nucleon respectively, and their ratios. Also we give the predictions for the angular distributions of the  $\pi$  in the  $\pi \Lambda$  c.m. system. Through the analysis, we find that the  $\Sigma^*(\frac{1}{2}^-)$  and the interference term of  $\Sigma^*(\frac{3}{2}^+)$  and  $\Sigma^*(\frac{1}{2}^-)$  play significant roles near threshold, such that the ratios of  $\sigma_{\frac{3}{2}}/\sigma_{\frac{1}{2}}$  and the angular distribution of the  $\pi$  are distinctly different assuming that the  $\Sigma^*(\frac{1}{2}^-)$  exists or not. The results of this work may be useful for identification of  $\Sigma^*(\frac{1}{2}^-)$  when the experimental data are available in the future.

#### Acknowledgements

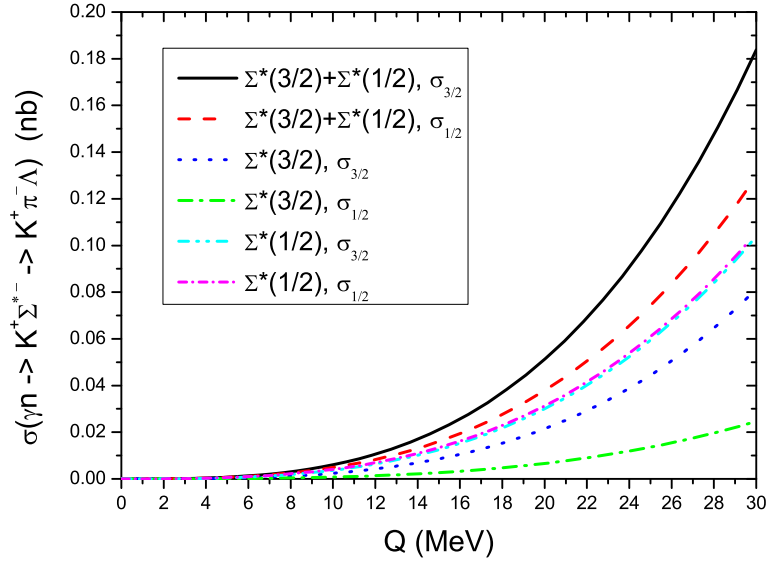
We acknowledge Eulogio Oset for the suggestion to start this work and carefully reading through the manuscript. We also thank Puze Gao, Jia-jun Wu and Jian-ping Dai for helpful discussions. This work is supported in part by the National Natural Science Foundation of China under Grant 11035006, 11121092, 11261130311 (CRC110 by DFG and NSFC), the Chinese Academy of Sciences under Project No.KJCX2-EW-N01 and the Ministry of Science and Technology of China (2009CB825200).

- 
- [1] C. Helminen and D. O. Riska, Nucl. Phys. A **699**, 624 (2002).
  - [2] B. S. Zou, Eur. Phys. J. A **35**, 325 (2008); Int. J. Mod. Phys. A **21**, 5552 (2006).
  - [3] B. C. Liu and B. S. Zou, Phys. Rev. Lett. **96**, 042002 (2006); Phys. Rev. Lett. **98**, 039102 (2007).
  - [4] C. S. An, Q. B. Li, D. O. Riska and B. S. Zou, Phys. Rev. C **74**, 055205 (2006) [Erratum-ibid. C **75**, 069901 (2007)].
  - [5] C. S. An, Nucl. Phys. A **797**, 131 (2007); Nucl. Phys. A **801**, 82 (2008).
  - [6] A. Zhang *et al.*, High Energy Phys. Nucl. Phys. **29**, 250 (2005).
  - [7] J. J. Wu, S. Dulat, and B. S. Zou, Phys. Rev. D **80**, 017503 (2009).
  - [8] J. J. Wu, S. Dulat, and B. S. Zou, Phys. Rev. C **81**, 045210 (2010).
  - [9] P. Z. Gao, J. J. Wu, and B. S. Zou, Phys. Rev. C **81**, 055203 (2010).

- [10] K. Moriya *et al.* [CLAS Collaboration], arXiv:1301.5000 [nucl-ex].
- [11] J. H. R. Crouch *et al.* (Cambridge Bubble Chamber Group), Phys. Rev. **156**, 1426 (1967).
- [12] R. Erbe *et al.* (DESY Bubble Chamber Group), Nuovo Cimento A **49**, 504 (1967).
- [13] R. Erbe *et al.* (ABBHHM Collaboration), Phys. Rev. **188**, 2060 (1969).
- [14] L. Guo and D. P. Weygand (CLAS Collaboration), in *Proceedings of the International Workshop on the Physics of Excited Baryons (NSTAR05)*, edited by S. Capstick, V. Crede, and P. Eugenio (World Scientific, Singapore, 2006, pp. 306-309.
- [15] K. Hicks *et al.* (LEPS Collaboration), Phys. Rev. Lett. **102**, 012501 (2009).
- [16] M. F. M. Lutz and M. Soyeur, Nucl. Phys. A **748**, 499 (2005).
- [17] M. Döring, E. Oset, and D. Strottman,, Phys. Lett. B **639**, 59 (2006); Phys. Rev. C **73**, 045209 (2006).
- [18] Y. Oh, C. M. Ko, and K. Nakayama, Phys. Rev. C **77**, 045204 (2008).
- [19] Y. Oh, K. Nakayama, and T.-S. H. Lee, Phys. Rep.**423**, 49 (2006).
- [20] J. Beringer *et al.* (Particle Data Group), Phys. Rev. D **86**, 010001 (2012).
- [21] D. B. Lichtenberg, Phys. Rev. D **15**, 345 (1977).
- [22] H. Haberzettl, K. Nakayama, and S. Krewald, Phys. Rev. C **74**, 045202 (2006).
- [23] P. Z. Gao, J. Shi, and B. S. Zou, Phys. Rev. C **86**, 025201 (2012).
- [24] J. D. Bjorken and S. D. Drell, *Relativistic Quantum Mechanics*, Graw-Hill, New York, 1965.

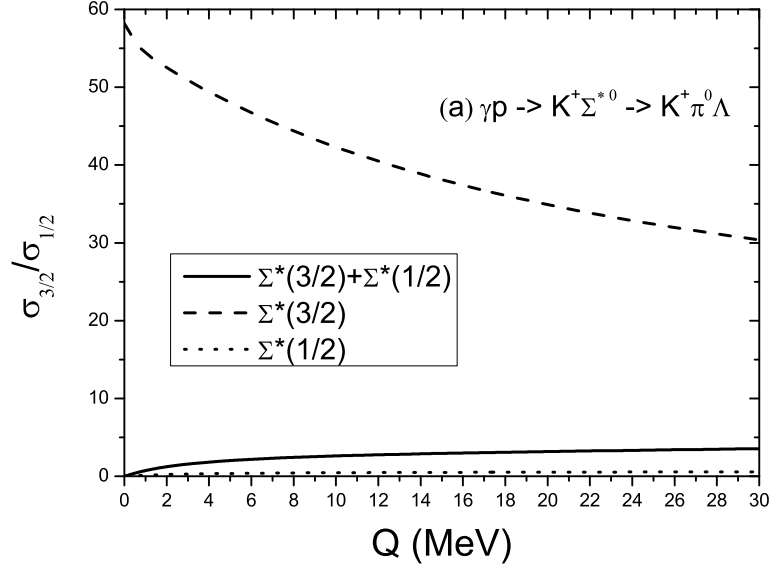


(a)

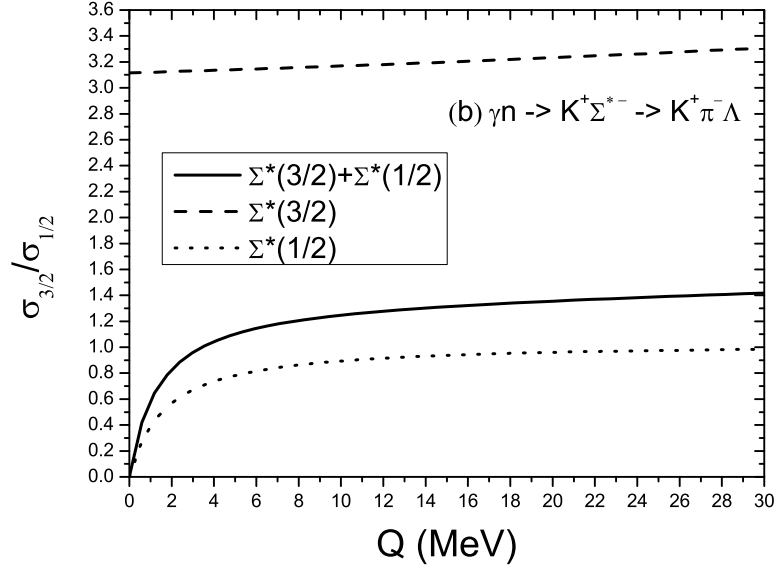


(b)

FIG. 2: Predictions for the helicity cross sections contributed from  $\Sigma^*(\frac{3}{2}^+)$ ,  $\Sigma^*(\frac{1}{2}^-)$  and the sum of them for (a)  $\gamma p \rightarrow K^+ \Sigma^{*0} \rightarrow K^+ \pi^0 \Lambda$  and (b)  $\gamma n \rightarrow K^+ \Sigma^{*-} \rightarrow K^+ \pi^- \Lambda$  processes, respectively.



(a)



(b)

FIG. 3: Predictions for the ratios of  $\sigma_{\frac{3}{2}}/\sigma_{\frac{1}{2}}$  assuming there exist only  $\Sigma^*(\frac{3}{2}^+)$  (dashed), or only  $\Sigma^*(\frac{1}{2}^-)$  (dotted) or both of them (solid) for (a)  $\gamma p \rightarrow K^+ \Sigma^{*0} \rightarrow K^+ \pi^0 \Lambda$  and (b)  $\gamma n \rightarrow K^+ \Sigma^{*-} \rightarrow K^+ \pi^- \Lambda$  processes, respectively.

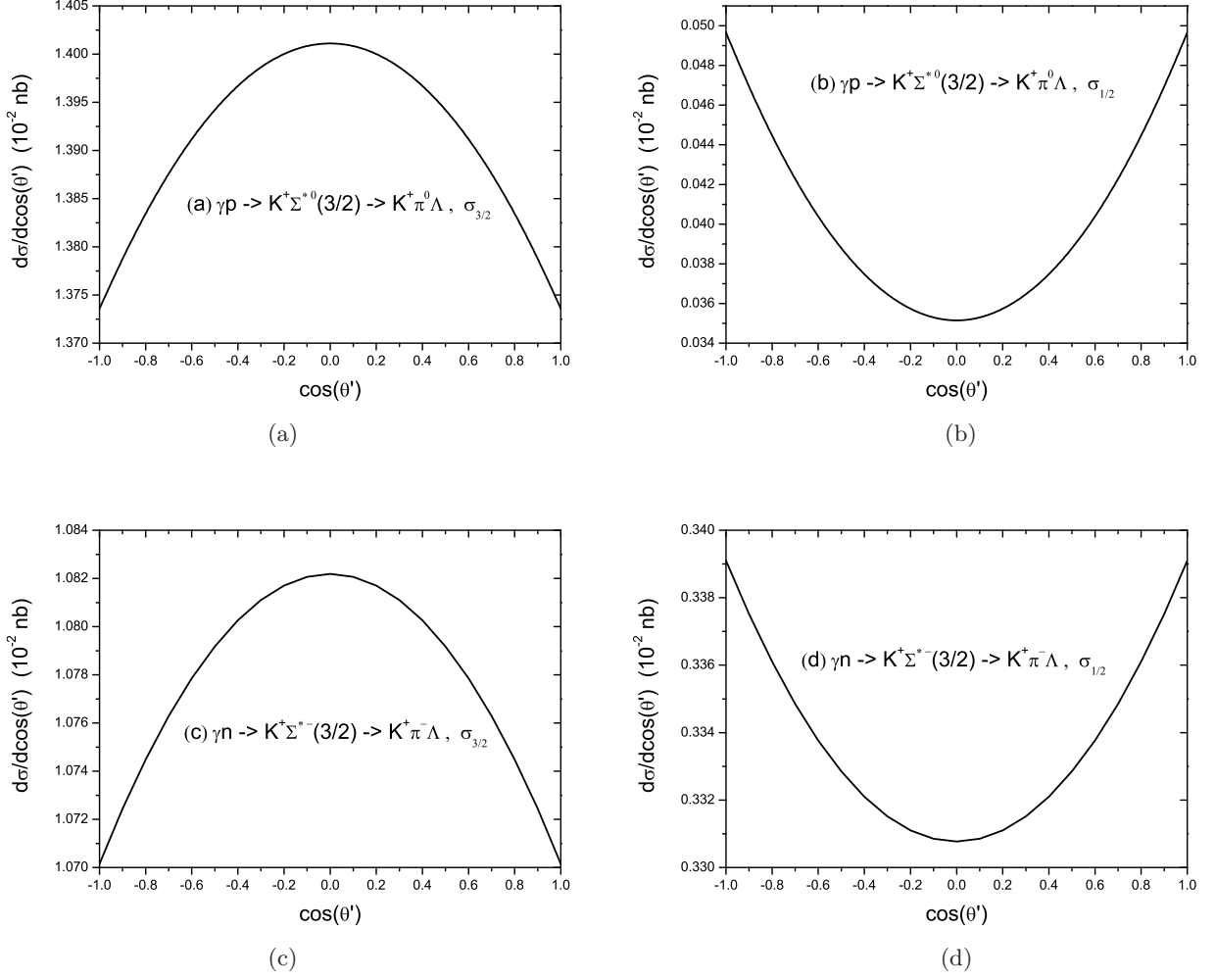


FIG. 4: Predictions for the angular distribution of final  $\pi$  of the  $\gamma N \rightarrow K^+ \Sigma^*(\frac{3}{2}^+) \rightarrow K^+ \pi \Lambda$  process, where  $\theta'$  is the angle between the outgoing  $\pi$  direction and  $K$  direction in the c.m. system of  $\pi \Lambda$ . (a) and (b) denote  $\sigma_{3/2}$  and  $\sigma_{1/2}$  respectively for  $\gamma p \rightarrow K^+ \Sigma^{*0}(\frac{3}{2}^+) \rightarrow K^+ \pi^0 \Lambda$  process. (c) and (d) denote  $\sigma_{3/2}$  and  $\sigma_{1/2}$  respectively for  $\gamma n \rightarrow K^+ \Sigma^{*-}(\frac{3}{2}^+) \rightarrow K^+ \pi^- \Lambda$  process.

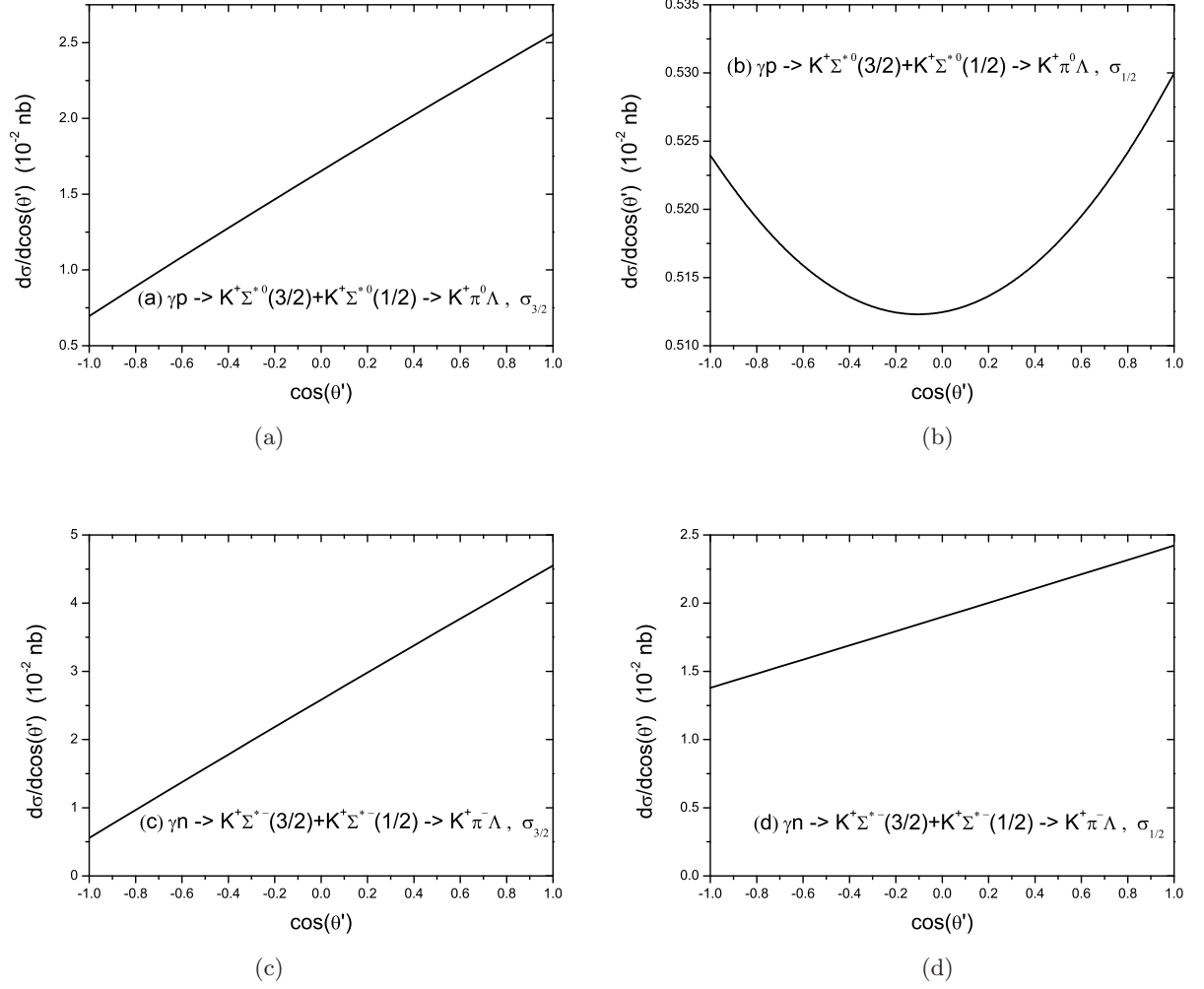


FIG. 5: Predictions for the angular distribution of final  $\pi$  of the  $\gamma N \rightarrow K^+ \Sigma^* \rightarrow K^+ \pi \Lambda$  process, where  $\Sigma^*$  include  $\Sigma^*(\frac{3}{2}^+)$  and  $\Sigma^*(\frac{1}{2}^-)$ . (a) and (b) denote  $\sigma_{3/2}$  and  $\sigma_{1/2}$  respectively for  $\gamma p \rightarrow K^+ \Sigma^{*0} \rightarrow K^+ \pi^0 \Lambda$  process. (c) and (d) denote  $\sigma_{3/2}$  and  $\sigma_{1/2}$  respectively for  $\gamma n \rightarrow K^+ \Sigma^{*-} \rightarrow K^+ \pi^- \Lambda$  process.